IOP Publishing Superconductor Science and Technology
Supercond. Sci. Technol. **27** (2014) 125003 (7pp) doi:10.1088/0953-2048/27/12/125003

Flux pinning mechanism in SiC and nano-C doped MgB_2: evidence for transformation from δT_c to $\delta \ell$ pinning

S R Ghorbani[1], G Farshidnia[2], X L Wang[3] and S X Dou[3]

[1] Department of Physics, Ferdowsi University of Mashhad, Mashhad, Iran
[2] Department of Physics, Hakim Sabzevari University, Sabzevar, Iran
[3] Institute for Superconducting and Electronic Materials, Australian Institute for Innovative Materials, Faculty of Engineering, University of Wollongong, North Wollongong, NSW 2519, Australia

E-mail: sh.ghorbani@um.ac.ir

Received 20 May 2014, revised 21 August 2014
Accepted for publication 19 September 2014
Published 31 October 2014

Abstract

Magnetic and transport properties of 10 wt% SiC doped MgB_2 and 5 wt% nano-C doped MgB_2 were studied by resistance and critical current density measurements. The results showed improvement of the critical current density for the MgB_2 superconductor doped with SiC in comparison with the nano-C doped sample. The flux pinning mechanisms of both doped MgB_2 superconductors have been investigated based on the collective theory. It was found that the pinning mechanism in MgB_2 was transformed by SiC doping from transition temperature fluctuation induced pinning, δT_c pinning, to mean free path fluctuation induced pinning, $\delta \ell$ pinning, while in the MgB_2 doped with nano-C, δT_c and $\delta \ell$ pinning coexist. Their contributions are strongly temperature dependent, however. The $\delta \ell$ pinning is dominant at low temperature, decreases with increasing temperature, and is suppressed completely at temperatures close to T_c. The δT_c pinning mechanism shows the opposite trend.

Keywords: flux pinning mechanism, critical current density, SiC doped MgB_2

(Some figures may appear in colour only in the online journal)

1. Introduction

The critical current density and the upper critical field, H_{c2}, have been central topics of much research since the discovery of superconductivity in magnesium diboride, MgB_2, with its superconducting transition temperature of $T_c \approx 39$ K [1]. MgB_2 is attractive for technical applications that require not only a high upper critical field, H_{c2}, but also need to carry a large supercurrent in the presence of high magnetic fields. High critical current density values of 10^5–10^6 A cm^{-2} and an upper critical field of roughly 40 T have been reported for this superconductor. It has already been shown that a J_c enhancement by more than one order of magnitude in high magnetic fields can be easily achieved with only slight reduction in T_c through adding nano-particles of C sources such as SiC [2–9] and carbohydrates [10, 11]. However, C sources mainly consist of carbon (C), oxygen (O), and hydrogen (H), so that the O can easily react with Mg to form MgO, which may enhance the vortex pinning, but it also strongly degrades the connectivity if present between MgB_2 grains, as seen in O-contaminated MgB_2 [12]. A large amount of MgO remains between the MgB_2 grains as insulating precipitates which reduces the effective superconducting cross-sectional area of the sample and thus blocks the supercurrent.

The main application problem for the MgB_2 superconductor is that the critical current density rapidly drops with increasing magnetic field due to its poor flux pinning. At the irreversibility field, H_{irr}, vortices start to move along the direction of the current flow, and hence the critical current vanishes. The current density decay behavior is governed by the pinning mechanism, which is still under investigation. Therefore, the vortices have to be pinned by flux pinning centers. Numerous studies have been performed with the

purpose of understanding the vortex-pinning mechanisms [2, 3, 13–24] that are responsible for improving the critical current density, J_c. Intergrain boundary pinning [19] and point defect pinning [16] are two main important pinning mechanisms.

Fluctuations in T_c and the mean free path of charge carriers control the flux pinning in high T_c superconductors are are two basic pinning mechanisms in type-II superconductors [25, 26]. The T_c distribution in the sample [5] is due to Mg deficiency and partial dopant substitution into the lattice leads to the T_c fluctuation in MgB_2. However, it is the inter-grain boundaries and the nanoparticle inclusions inside the MgB_2 grains that cause the mean free path fluctuations and hence the δl pinning. It has been reported that the δT_c pinning is the main flux pinning mechanism in pure MgB_2 bulk [17]. It was found that both pinning mechanisms coexist in the nanoparticle doped-MgB_2 samples, depending on the temperature [15, 18, 24].

The upper critical field H_{c2} in MgB_2 has been significantly enhanced using various approaches, including high energy ion irradiation [27], chemical substitutions, and incorporation of nano-particles such as nano-SiC, C, and Si, as well as other oxide or non-oxide nano-materials [2, 3, 14, 21–24]. It has been accepted that for chemical doping that contains C, the enhancement of the H_{c2} is caused by the C substitution for B in the crystal lattice. The mean free path ℓ is reduced due to the distortion in the lattice caused by the C substitution. Therefore, the σ band electron scattering is enhanced and leads to the increase in H_{c2} and a large decrease in T_c, which is a disadvantage for application at $T > 20$ K. It should be noted that substitution may not take place in MgB_2 doped with non-carbon-based nano-particles, which can also improve the H_{c2}. Nano-Si has been found to be very effective for significantly improving the J_c in both low and high fields with slightly reduced T_c, although no Si substitution takes place [3]. The J_c values at temperatures above 20 K for the nano-Si doped MgB_2 were found to be even higher than for the C-doped MgB_2 [3]. It has been found that MgB_2 doped with SiC has the weakest J_c field dependence of at 20 K when compared with Si or C [3, 4, 28]. Such a superior field performance is an indication of the combined effects of C doping and flux pinning by defects and nano-precipitates [4]. In SiC doped MgB_2, the C source for doping is typically from the reaction between SiC and MgB_2 to form Mg_2Si [5], leaving behind the C, which in the presence of B, reacts with Mg to form $Mg(B_{1-x}C_x)_2$. Improvement of the $J_c(B)$ has been quite successful for most chemically doped MgB_2 (such as with nano-C, Si, or SiC). The origin of the pinning mechanisms is still not well understood, however. Therefore, explanations of the pinning mechanisms are of interest from the point of view of both the fundamental physics and applications, especially for MgB_2 doped with nano-C and other chemical dopants that contains both C and Si.

In spite of intensive studies on pinning and J_c enhancement in SiC doped MgB_2 over the last 13 years, the pinning mechanism on why SiC doping is unique still remains unclear. Moreover, it has been believed that the C substitution for boron enhances H_{c2} while the defects and grain boundaries are responsible for flux pinning. The question is whether there is any common ground for the effect of SiC and C dopants on the flux pinning in MgB_2? To answer these questions, we have conducted a systematic study on the pinning mechanisms in MgB_2 doped with two C-source such as C and SiC and roughly same critical temperature, T_c. The vortex-pinning mechanisms of these dopants are analyzed in the framework of the collective theory. It has been found that there is competition between charge carrier mean free path fluctuation pinning ($\delta\ell$) and pinning due to spatial variations of the transition temperature (δT_c pinning) for the nano-C doped MgB_2 sample, while the pinning mechanism in the SiC doped sample is $\delta\ell$.

2. Experimental procedure

Polycrystalline MgB_2 samples with 10 wt% SiC and with 5 wt% nano-C were prepared at the sintering temperature of 800 °C by the standard solid-state powder processing technique, which has been well described elsewhere [6]. A pure MgB_2 sample was also prepared by the same method as a reference. The critical temperature T_c was defined as the onset temperature at which diamagnetic properties were observed. T_c was 36.8 and 35.6 K for the two doped samples, respectively. The x-ray diffraction (XRD) patterns of the samples were collected using Cu Kα radiation. The resistivity measurements were carried out by using a physical properties measurement system (PPMS, Quantum Design) in the field range from 0 up to 8.7 T. The magnetic hysteresis loops were measured using a magnetic properties measurement system (MPMS; Quantum Design) in the field range from 0–5 T and temperature from 20–33 K. The critical current density was calculated by using the Bean approximation, $J_c = 20\Delta M/Vw(1 - w/3l)$, where w and l are the width and the length of the sample perpendicular to the applied field, respectively, with $w \leqslant l$, V is the sample volume, and ΔM is the height of the M-H hysteresis loop.

3. Results and discussion

XRD patterns for the pure and both doped MgB_2 samples are shown in figure 1, which revealed that all the samples were crystallized in the MgB_2 structure as the major phase. As can be seen in figure 1, a few impurity lines of MgO are visible in the pure reference sample and in both doped samples, as well as lines for Mg_2Si in the SiC doped sample. The estimated fractions of MgO and Mg_2Si were roughly 5 and 10%, respectively, that is in agreement with the impurity amounts reported before [29]. From energy dispersive spectroscopy (EDS) [2], it was found that the Mg:Si ratio was uniform over the entire area, indicating a homogeneous phase distribution. The (100) peak is slightly shifted towards higher angles, indicating a decrease in the a lattice parameter, which suggested C substitution on B sites for both doped samples. These observations were further explained by the T_c values, to be discussed later. The (002) peak reflects the c lattice

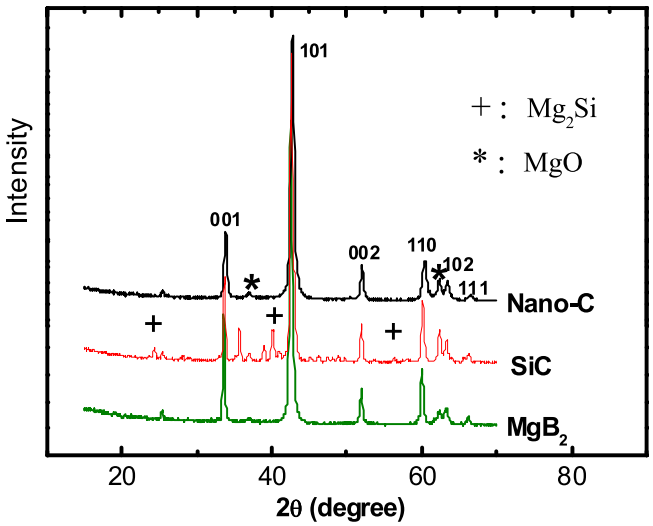

Figure 1. X-ray diffraction pattern of the pure, and the SiC and nano-C doped MgB_2 samples.

parameter. The position of this peak does not change noticeably, and consequently, c does not change.

The lattice parameters were calculated from the XRD patterns. For the pure sample, a and c were 3.080 and 3.520 Å, while a was 3.071 Å and 3.060 Å for the SiC and the nano-C doped MgB_2 samples, respectively, and c was 3.517 Å for both doped samples. The decrease in the a lattice parameter is quite pronounced, while the c-parameter is constant. The change in this lattice parameter confirms the partial replacement of boron by carbon. The level of C substitution, x in the formula $Mg(B_{1-x}C_x)_2$, can be estimated as $x = 7.5 \times \Delta(c/a)$, where $\Delta(c/a)$ is the change in c/a compared to a pure sample [7]. It was found that the x value was 0.017 and 0.048 for the SiC doped and the nano-C doped MgB_2 samples, respectively, suggesting that C substitution on B sites for the nano-C doped sample was larger than that for the SiC.

The amount of carbon substituted into B sites in our samples was estimated based on the reduction in the lattice parameter a. Our data is in agreement with the correlation between the a lattice parameter and C substitution level reported by Kazakov *et al* [8]. It was found that the T_c and the a lattice parameter decrease monotonically with increasing carbon content in $Mg(B_{1-x}C_x)_2$ single crystals with $0 \leqslant x \leqslant 0.10$ and decrease faster for $x > 0.10$. Therefore, it is true that the low T_c of 35.6 K is caused by C doping.

The H_{c2} and H_{irr} are determined from the 90% and 10% drop, respectively, at the transition in the normal-state resistivity values in the R-T curves. The H_{c2} and H_{irr} as functions of the normalized temperature T/T_c are shown in figure 2. The R-T curves as functions of magnetic field are shown in the inset of figure 2(a) for both the SiC and the nano-C doped MgB_2. As can be seen in the inset of figure 2(a), the critical temperature T_c suppress with increasing magnetic field. The T_c of the nano-C doped sample is smaller than that for the SiC doped sample by roughly 1 K at zero magnetic field. This indicates further C substitution for C in the nano-C doped sample, which is also supported by the greater decrease in the

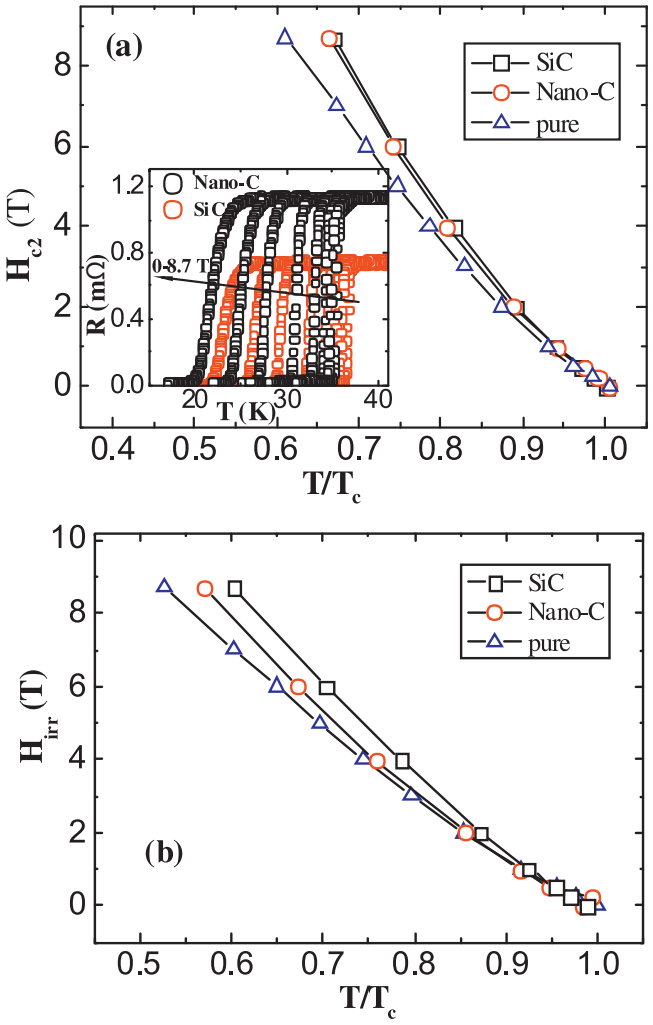

Figure 2. (a) The upper critical and (b) the irreversibility fields of the pure, the 10 wt% SiC doped, and the 5 wt% nano-C doped MgB_2 as functions of temperature. Inset (a): the resistance of both doped MgB_2 samples as functions of the temperature and magnetic field.

a lattice parameter, as mentioned above. The H_{c2} and H_{irr} values of the undoped sample are also included in figure 2 for comparison. The upper critical field value at 25 K for the undoped sample is about 7 T, while the values for both the SiC and the nano-C doped samples at the same temperature are 8.7 T. As can be seen in figure 2(b), the H_{irr} results reveal that although both the nano-C doped and the SiC doped MgB_2 show improved H_{irr} values compared to the undoped sample, the SiC doped MgB_2 shows the most significant enhancement. The inclusion of the SiC in the doped MgB_2 results in two effects. The first is the partial substitution for B by C released from the SiC, which may induce disorder on the lattice sites and result in the enhancement of both H_{irr} and H_{c2}. The second effect is that the formation of Mg_2Si can introduce point defects and affect the grain boundaries. This result is in agreement with the XRD results, as shown above, and what has been previously reported [3]. Both effects reduce the mean free path, ℓ, which can lead to enhancement of the H_{irr} and H_{c2}. The latter effect may be responsible for

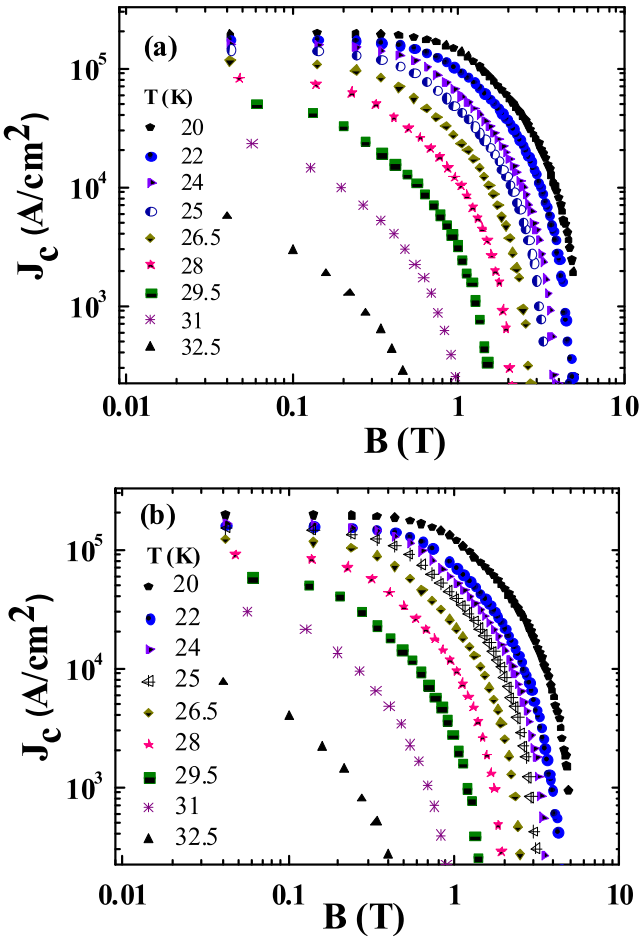

Figure 3. Magnetic and temperature dependences of the critical current density for (a) the SiC doped MgB_2 and (b) the nano-C doped MgB_2 superconductor.

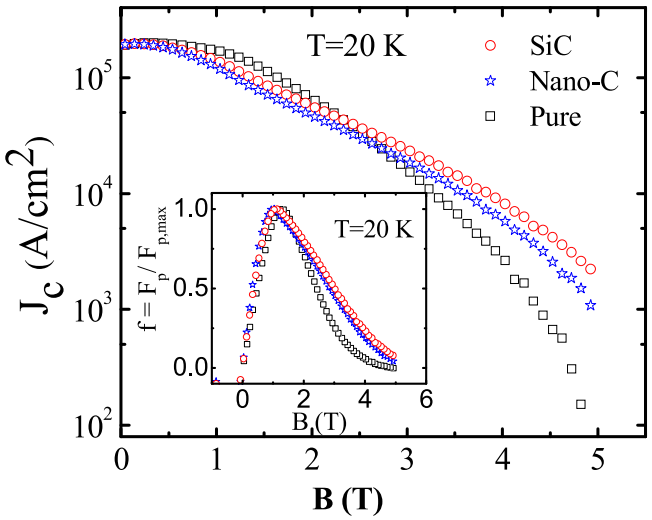

Figure 4. Critical current density for the pure, the 10 wt% SiC doped, and the 5 wt% nano-C doped MgB_2 samples as a function of magnetic field at the temperature of 20 K. Inset: The magnetic field dependence of the normalized volume pinning force ($f = F_p/F_{p,max}$).

the significant enhanced H_{irr} for the SiC doped MgB_2 compared to the nano-C doped sample.

Magnetic hysteresis loops were collected in the temperature range of 20–32.5 K for both the SiC doped and the nano-C doped MgB_2 samples. The critical current density was calculated by using the Bean critical model. Figure 3 shows the magnetic field dependence and the temperature dependence of the J_c for both doped MgB_2 samples. For comparison purposes, the J_c values at 20 K for both the SiC and the nano-C doped MgB_2 samples and the pure MgB_2 sample are plotted in figure 4. The J_c at 20 K for both the SiC and the nano-C doped MgB_2 samples at high fields are higher than for the pure MgB_2 sample, which was made under the same conditions as the doped MgB_2 samples. As can be seen from figure 4, the J_c is very much enhanced in high magnetic fields for both the SiC doped and the nano-C doped MgB_2 samples. The SiC dopant increases the J_c value by more than an order of magnitude over that for the undoped MgB_2 at $T = 20$ K and $B = 4.5$ T. Therefore, the SiC doped MgB_2 exhibits significantly improved pinning in high fields over a wide temperature range compared with the pure MgB_2 and the nano-C doped MgB_2 samples. In low magnetic fields, however, the J_c of the SiC and nano-C doped MgB_2 and undoped sample are the same and sometimes it is smaller for doped samples. From transmission electron microscopy (TEM) investigations [9], it was found that SiC doping allowed the creation of intragrain defects and highly dispersed nano-inclusions such as Mg_2Si and MgO within the grains. These nano-inclusions are responsible for two effects. The first one is that the amount of MgB_2 phase is accordingly decreased, which decreases the effective superconducting volume in the doped samples. This effect results in J_c reduction in low fields. The second effect is the formation of nano-sized pinning centers, which improves J_c-H behavior in high magnetic fields.

The J_c of the SiC sample is larger than that of the nano-C sample at high temperature over the entire range of magnetic field. As mentioned above, the SiC doped MgB_2 sample contains induced Mg_2Si impurity phase. This indicates that there is degradation of the crystallinity of the SiC sample due to the Mg_2Si inclusions within the grain boundaries, resulting in the introduction of point defects. Flux pinning by point defects is the dominant factor for J_c at high magnetic field, however. Therefore, more pinning centers were introduced in the SiC doped MgB_2 sample than in the nano-C sample, which resulted in better $J_c(B)$ performance at high magnetic fields.

To study the pinning properties of both doped MgB_2 samples, the volume pinning force $F_p = J_c \times B$ was calculated for both samples. For comparison of the volume pinning force, the magnetic field dependence of the normalized pinning force ($f = F_p/F_{p,max}$), where $F_{p,max}$ is the maximum value of F_p, is shown in the inset of figure 4 for all three samples at 20 K. As can be seen, the values of the $f(B)$ curves are different at high magnetic fields for SiC and C dopant. A higher value indicates higher pinning strength. At B = 3.5 T, the f is 0.12 for undoped MgB_2 and over 0.29 and 0.35 for nano-C and SiC doped MgB_2, respectively. Therefore, the SiC doping leads to a higher value for the volume pinning force than that

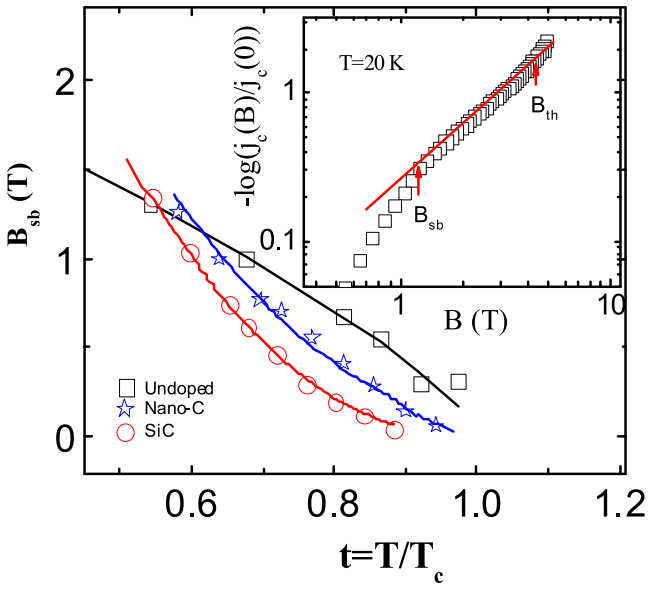

Figure 5. Temperature dependence of the crossover field B_{sb}. The solid curves are fits to equation (4). Inset: double logarithmic plot of $-\log[J_c(B)/J_c(0)]$ as a function of B at $T = 20$ K for the MgB_2 doped with SiC. The crossover fields B_{sb} and B_{th} (to the thermal regime) are shown by arrows.

for nano-C doping and undoped samples, this result in strong pinning and thus larger J_c.

The collective theory [26] was used to analyze the vortex-pinning mechanisms of these dopants. According to this theory, J_c is field independent at magnetic fields lower than the crossover field, B_{sb}, which marks the transition from the single vortex to the small bundle pinning regime. Below this regime, single vortex pinning governs the vortex lattice:

$$B_{sb} \propto J_{sv} B_{c2}, \tag{1}$$

where J_{sv} is the critical current density in the single vortex pinning regime. At higher fields, $B > B_{sb}$, $J_c(B)$ decreases quickly, and it follows an exponential law:

$$J_c(B) \approx J_c(0) \cdot \exp\left[-\left(B/B_0\right)^{3/2}\right], \tag{2}$$

where B_0 is a normalization parameter on the order of B_{sb}. At higher magnetic fields, a power dependence in the form of $J_c \propto B^{-\beta}$, where β is a parameter, acts from B_{sb} up to another crossover field, B_{lb} (to the large bundle pinning regime).

For clarification, $-\log[J_c(B)/J_c(0)]$ as a function of B is shown in a double logarithmic plot in the inset of figure 5. It is clear that this expression well describes the experimental data for intermediate fields, while deviations from the fitting curves can be observed at both low and high fields. The deviation at low fields is associated with a crossover from the single-vortex-pinning regime to the small-bundle-pinning regime. The crossover field B_{sb} as a function of temperature is shown in figure 5. As a comparison, the B_{sb} results for the undoped MgB_2 sample are also shown in the figure, which displays a different trend from that of the doped samples.

It is believed that the fluctuations in the T_c and in the mean free path of the charge carriers both control the flux pinning in high T_c superconductors [17, 30]. Partial doping substitution and Mg deficiency are the two main reasons for the T_c fluctuation, while the mean free path fluctuation, and hence the $\delta\ell$ pinning, is caused by the intergrain boundaries and intergrain inclusions. For MgB_2 superconductor, it has been shown that δT_c pinning is dominant in undoped MgB_2 samples, while both δT_c and $\delta\ell$ pinning mainly coexist in carbon-containing doped MgB_2 bulk samples [15, 18, 24].

It has been pointed out [28] that the δT_c and $\delta\ell$ pinning mechanisms result in different temperature dependence of the critical current density J_{sv} in the single vortex pinning regime. For δT_c pinning, $J_{sv} \propto \left(1 - t^2\right)^{7/6}\left(1 + t^2\right)^{5/6}$, with $t = T/T_c$, while for the case of $\delta\ell$ pinning, $J_{sv} \propto \left(1 - t^2\right)^{5/2}\left(1 + t^2\right)^{-1/2}$. In the single-vortex-pinning region the following B_{sb} temperature dependence can be obtained [17]:

$$B_{sb} = B_{sb}(0)\left(\frac{1 - t^2}{1 + t^2}\right)^{\nu}, \tag{3}$$

where the parameter $\nu = 0.67$ and 2 for δT_c and $\delta\ell$ pinning, respectively.

It was found that there is no agreement between the experimental data for the doped MgB_2 and equation (3) with $\nu = 2$ or 0.67 [15, 18], and that strongly suggests that the δT_c and the $\delta\ell$ pinning mechanisms coexist in our samples. The $\delta\ell$ and δT_c pinning mechanisms are the main pinning mechanism. Both play as pinning role in C-source doped MgB_2 [15, 18, 24]. Therefore, to investigate the real pinning mechanisms of the doped MgB_2 samples, the B_{sb} data was analyzed by considering of coexistence both pinning mechanisms using the following expression [15, 18]:

$$B_{sb} = P_1 B_{sb}^{T_c} + P_2 B_{sb}^{l}, \tag{4}$$

where $B_{sb}^{T_c}$ and B_{sb}^{l} are the expressions for δT_c and $\delta\ell$ pinning, respectively. Parameter P_1 and P_2 reflects the weighting of the δT_c and $\delta\ell$ pinning mechanism. The B_{sb} data obtained from $J_c(B)$ is well described by equation (4), as shown by the solid curves in figure 5. The best-fitted value of $B_{sb}^{T_c}(0)$ and $B_{sb}^{l}(0)$ are 4.53 T and 1.97 T for the SiC-doped MgB_2 and the undoped MgB_2, respectively. They were also 0.75 T and 3.29 T for the nano-C doped MgB_2, respectively.

In order to consider both pinning mechanisms and compare the effects of the δT_c and $\delta\ell$ pinning mechanisms, the P parameter was defined as $P_{T_c} = P_1 B_{sb}^{T_c}/B_{sb}$ or $P_l = P_2 B_{sb}^{l}/B_{sb}$, which represent the δT_c or $\delta\ell$ pinning effects, respectively. The results for the contributions of both pinning effects are shown in figure 6. As can be seen in figure 6, the $\delta\ell$ pinning is the dominant mechanism for the SiC sample over the whole studied temperature range, due to the fine particles of Mg_2Si that are responsible for the $\delta\ell$ pinning. The transformation from the δT_c pinning to $\delta\ell$ pinning is in good agreement with the increasing resistivity. That is, with

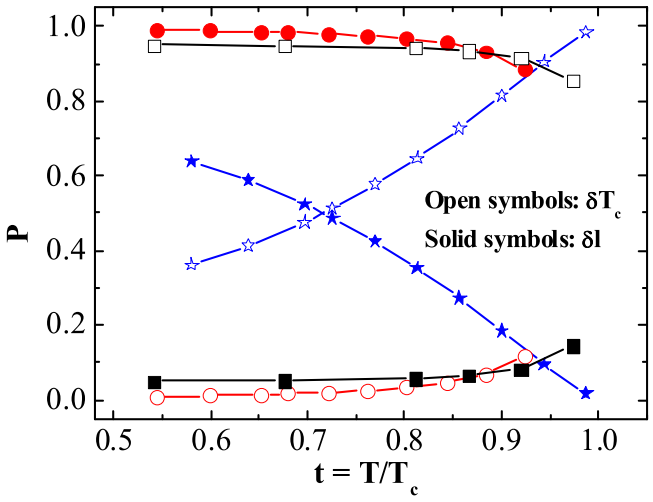

Figure 6. δT_c pinning and $\delta\ell$ pinning mechanism contributions as functions of temperature for pure (squares), 10 wt% SiC doped (circles), and 5 wt% nano-carbon doped MgB_2 (stars).

increasing resistivity, the electron scattering becomes stronger, thereby decreasing the charge carrier mean free path and increasing the $\delta\ell$ pinning.

For the nano-C sample, the δT_c pinning and $\delta\ell$ pinning mechanism coexist, and there is a competition between δT_c pinning and $\delta\ell$ pinning. $\delta\ell$ pinning is the dominant mechanism at low temperature, but with increasing temperature, $\delta\ell$ pinning decreases, and δT_c pinning increases. The temperature T_{eq} where both pinning mechanisms have equal effects is 26 K for the nano-C sample. In contrast, the δT_c pinning is the dominating mechanism over the whole temperature range for the undoped MgB_2 sample, which is partially due to the Mg deficiency from the formation of MgO impurity phase, in agreement with the XRD results. Therefore, the only Mg deficiency in nano-C doped MgB_2 samples leads to a broad distribution of T_c and thus is responsible for the δT_c pinning mechanism. While in SiC-doped MgB_2, the formation of Mg_2Si impurities inside grain is responsible for δl flux pinning and at the same time, it increases the mean-sized pinning centers, which improves J_c-H behavior in high magnetic fields.

In conclusion, we observed enhancements in the upper critical field, the irreversibility field, and the critical current density of both the SiC doped and the nano-C doped MgB_2 samples. These results provide strong evidence that the SiC produced very strong pinning centers, which enhanced $J_c(B)$ at high magnetic fields. On comparing with the collective pinning theory, the observed temperature dependence of the crossover field, $B_{sb}(T)$, from the single-vortex to the small-vortex-bundle pinning regime shows that $\delta\ell$ pinning is the dominant mechanism for the SiC sample over the whole studied temperature range. Therefore, the pinning mechanism in MgB_2 was transformed by SiC doping from the δT_c pinning to the $\delta\ell$ pinning mechanism, while the δT_c pinning and $\delta\ell$ pinning mechanisms coexist and there is a competition between δT_c pinning and $\delta\ell$ pinning for the nano-C sample.

Acknowledgments

The work was supported by the Ferdowsi University of Mashhad and the Australian Research Council.

References

[1] Nagamatsu J, Nakagawa N, Muranaka T, Zenitani Y and Akimitsu J 2001 *Nature* **410** 63
[2] Dou S X, Soltanian S, Horvat J, Wang X L, Zhou S H, Ionescu M, Liu H K, Munroe P and Tomsic M 2002 *Appl. Phys. Lett.* **81** 3419
[3] Wang X L, Zhou S H, Qin M J, Munroe P R, Soltanian S, Liu H K and Dou S X 2003 *Physica* C **385** 461
Wang X L, Soltanian S, James M, Qin M J, Horvat J, Yao Q W, Liu H K and Dou S X 2004 *Physica* C **408–410** 63
[4] Serrano G, Serquis A, Dou S X, Soltanian S, Civale L, Maiorov B, Holesinger T G, Balakirev F and Jaime M 2008 *J. Appl. Phys.* **103** 023907
[5] Dou S X *et al* 2007 *Phys. Rev. Lett.* **98** 097002
[6] Kim J H, Dou S X, Hossain M S A, Xu X, Wang J L, Shi D Q, Nakane T and Kumakura H 2007 *Supercond. Sci. Technol.* **20** 715
[7] Avdeev M, Jorgensen J D, Ribeiro R A, Bud'ko S L and Canfield P C 2003 *Physica* C **387** 301
[8] Kazakov S M, Puzniak R, Rogacki K, Mironov A V, Zhigadlo N D, Jun J, Soltmann C, Batlogg B and Karpinski J 2005 *Phys. Rev.* B **71** 024533
[9] Dou S X, Pan A V, Zhou S, Ionescu M, Wang X L and Munroe P R 2003 *J. Appl. Phys.* **94** 1850
[10] Kim J H, Zhou S, Hossain M S A, Pan A V and Dou S X 2006 *Appl. Phys. Lett.* **89** 142505
[11] Hossain M S A, Kim J H, Wang X L, Peleckis G and Dou S X 2007 *Supercond. Sci. Technol.* **20** 112
[12] Gao Z, Ma Y, Zhang X, Wang D, Yu Z, Watanabe K, Yang H and Wen H 2007 *Supercond. Sci. Technol.* **20** 485
[13] Larbalestier C *et al* 2001 *Nature* **410** 186
[14] Liao X Z, Serquis A C, Zhu Y T, Huang J Y, Peterson D E, Mueller F M and Xu H F 2002 *Appl. Phys. Lett.* **80** 4398
[15] Ghorbani S R, Wang X L, Dou S X, Lee S-I and Hossain M S A 2008 *Phys. Rev.* B **78** 184502
[16] Dou S X, Wang X L, Horvat J, Milliken D, Collings E W and Sumption M D 2001 *Physica* C **361** 79
[17] Qin M J, Wang X L, Liu H K and Dou S X 2002 *Phys. Rev.* B **65** 132508
[18] Ghorbani S R, Wang X L, Hossain M S A, Yao Q W, Dou S X, Lee S-I, Chung K C and Kim Y K 2010 *J. Appl. Phys.* **107** 113921
[19] Lee S, Mori H, Masui T, Eltsev Y, Yamamoto A and Tajima S 2001 *J. Phys. Soc. Japan* **70** 2255
[20] Dou S X, Yeoh W K, Horvat J and Ionescu M 2003 *Appl. Phys. Lett.* **83** 4996
[21] Eisterer M, Zehetmayer M, Tonies S, Weber H W, Kambara M, Babu N H, Cardwell D A and Greenwood L R 2002 *Supercond. Sci. Technol.* **15** L9
[22] Yamada H, Hirakawa M, Kumakura H and Kitaguchi H 2006 *Supercond. Sci. Technol.* **19** 179
[23] Ma Y W, Zhang X P, Nishijima G, Watanabe K, Awaji S and Bai X D 2006 *Appl. Phys. Lett.* **88** 072502
[24] Ghorbani S R, Wang X L, Hossain M S A, Dou S X and Lee S-I 2010 *Supercond. Sci. Technol.* **23** 025019
[25] Blatter G, Feigel'man M V, Geshkenbein V B, Larkin A I and Vinokur V M 1994 *Rev. Mod. Phys.* **66** 1125
[26] Griessen R, Hai-hu W, van Dalen A J, Dam B, Rector J and Schnack H G 1994 *Phys. Rev. Lett.* **72** 1910

[27] Bugoslavsky Y, Cohen L F, Perkins G K, Polichetti M, Tate T J and Gwilliam Rand Caplin A D 2001 *Nature* **411** 561
[28] Dou S X, Braccini V, Soltanian S, Klie R, Zhu Y, Li S, Wang X L and Larbalestier D 2004 *J. Appl. Phys.* **96** 7549
[29] Dou S X, Soltanian S, Horvat J, Wang X L, Zhou S H, Ionescu M and Liu H K 2002 *Appl. Phys. Lett.* **81** 3419
[30] Prischepa S L, Della Rocca M L, Maritato L, Salvato M, Capua R D, Maglione M G and Vaglio R 2003 *Phys. Rev.* B **67** 024512